2019

Colorimetric Detection of Aliphatic Alcohols in β-Cyclodextrin Solutions

Anna Haynes

Priva Halpert

Mindy Levine

ACS OMEGA

Article

Cite This: ACS Omega 2019, 4, 18361−18369

http://pubs.acs.org/journal/acsodf

Colorimetric Detection of Aliphatic Alcohols in β-Cyclodextrin Solutions

Anna Haynes,[†] Priva Halpert,[‡] and Mindy Levine*[,†,§]

[†]Department of Chemistry, University of Rhode Island, 140 Flagg Road, Kingston, Rhode Island 02881, United States

[‡]Stella K. Abraham High School for Girls, 291 Meadowview Ave, Hewlett, New York 11557, United States

Supporting Information

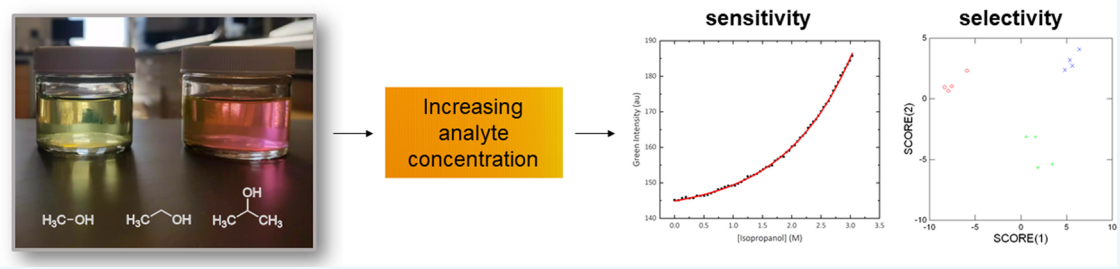

ABSTRACT: The sensitive, selective, and practical detection of aliphatic alcohols is a continuing technical challenge with significant impact in public health research and environmental remediation efforts. Reported herein is the use of a β-cyclodextrin derivative to promote proximity-induced interactions between aliphatic alcohol analytes and a brightly colored organic dye, which resulted in highly analyte-specific color changes that enabled accurate alcohol identification. Linear discriminant analysis of the color changes enabled 100% differentiation of the colorimetric signals obtained from methanol, ethanol, and isopropanol in combination with BODIPY and Rhodamine dyes. The resulting solution-state detection system has significant broad-based applicability because it uses only easily available materials to achieve such detection with moderate limits of detection obtained. Future research with this sensor system will focus on decreasing limits of detection as well as on optimizing the system for quantitative detection applications.

INTRODUCTION

Increased interest in using non-mass spectrometry-based techniques for the detection of small organic compounds has arisen due to practical challenges associated with the use of mass spectrometry that limit broad-based applicability.[1] Such challenges include the fact that expensive, bulky instrumentation is often required to accomplish mass spectrometry-based detection combined with significant user training to operate the instrumentation effectively, which prevents detection by relatively untrained citizen scientists.[2] Many newly developed chemosensors have focused on systems that allow for portable, on-site testing of the target analytes without requiring high-end, costly laboratory instrumentation.[3] A challenging aspect of designing portable chemosensors is the need to maintain high selectivity, sensitivity, and broad-based applicability in the efficient detection of various analytes, especially among analytes that are similar in structure and size.

By utilizing the ability of cyclodextrin to act as a supramolecular scaffold that facilitates proximity-induced, highly analyte-specific interactions between an analyte of interest and a high-quantum yield fluorophore, the Levine group has developed sensitive and selective fluorescence-based systems for analyte detection.[4,5] The systems utilize cyclodextrin-promoted fluorescence energy transfer from an analyte to a high quantum yield fluorophore for photophysically active analytes[6] or cyclodextrin-promoted, analyte-specific fluorescence modulation for nonphotophysically active analytes.[7] In addition to monitoring the analyte-specific fluorescence changes, there are often analyte-specific color changes in the fluorophore, promoted through the cyclodextrin-assisted interaction of the brightly colored fluorophore and the target analyte.[8] Advantages of colorimetric detection include the fact that the color changes can be easily detected using naked eye detection[9] or RGB analysis.[10] Significant literature precedent indicates that colorimetric analysis can be optimized for the detection of very small concentrations of toxicants both in solution-state and in solid-state detection devices.[11−13]

Colorimetric detection has potential utility in the detection of aliphatic alcohols, a class of analytes commonly found in commercial products that can cause health concerns, especially at elevated concentrations.[14] These alcohols, including isopropanol, ethanol, and methanol, are found in household cleaners,[15] paints,[16] self-care and beauty products,[17] and beverages.[18] Moreover, the need for aliphatic alcohol detection is rising with the increasing prevalence of at-home beer and alcohol production.[19] With almost no regulation of this process

Received: August 13, 2019
Accepted: October 10, 2019
Published: October 22, 2019

DOI: 10.1021/acsomega.9b02612
ACS Omega 2019, 4, 18361−18369

currently in place, there is significant potential for poorly controlled ethanol concentrations[20] as well as the potential for methanol contamination and associated methanol toxicity.[21] Furthermore, the brewing process can sometimes lead to the formation of other byproducts, including *n*-propanol, isobutanol, and isoamyl alcohol.[22] Because methods to detect these byproducts are not widely available, significant public health risks from their ingestion remain.[23] Additional potential applications of colorimetric aliphatic alcohol detection include the use of a colorimetric device to detect alcohol intoxication in both medical[24] and law-enforcement settings.[25] Finally, forensic analyses would benefit from the detection of a range of aliphatic alcohols that are known bacterial byproducts and could provide important forensic information.[26]

Previous reports on the detection of aliphatic alcohols by colorimetric methods include the use of a single ionic liquid, containing a modified pH indicator, to distinguish between eight aliphatic alcohols[27] as well as copper-containing metal−organic frameworks[28] and iron complexes[29] to accomplish effective detection. Cyclodextrins have also been reported in isolated instances to act as sensors for aliphatic alcohols through the use of cyclodextrin-based stationary phases in chiral chromatography[30] as well as through the use of a quartz crystal microbalance coated with cyclodextrin-derived compounds.[31] To the best of our knowledge, the combination of cyclodextrin-based complexation and colorimetric detection has not been reported to date.

While the fluorescence modulation method used previously in the Levine group provided good sensitivity and high selectivity among structurally similar analytes, it required laboratory-grade instrumentation, which severely limits widespread usage. Although portable fluorimetry has been accomplished using smartphone-based systems,[32] these systems can be challenging for the user to implement, which means that portable colorimetric systems can have notable advantages. Reported herein is the development of an extremely practical colorimetric detection system for isopropanol, ethanol, and methanol, based on color changes in a dye−cyclodextrin association complex upon addition of the aliphatic alcohol, with such color changes intimately dependent on the structure of each of the alcohols (structures **1**−**3**, Figure 1) and its association with both the cyclodextrin scaffold and

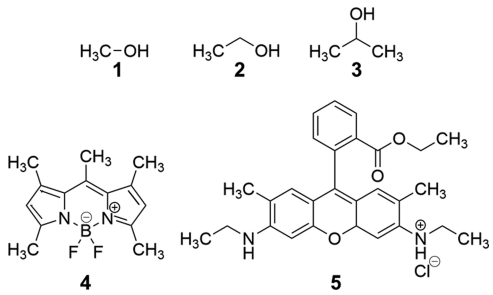

Figure 1. Structure of alcohol analytes (**1**−**3**) and highly colored dyes (**4** and **5**).

the colorimetric dye (BODIPY (**4**) or Rhodamine 6G (**5**), Figure 1). This system is highly robust with alcohol-induced color changes detectable even by a high school student working with unpurified tap water solutions and, even in its optimized formulation, uses no laboratory-grade instrumentation. Rather, the system uses a spray-painted plastic box equipped with LED lights to facilitate consistent coloration and enable reproducible results.

RESULTS AND DISCUSSION

Selection of Data Processing and Analytical Methods. Separation of the signals obtained from the photographs was performed using linear discriminant analysis (LDA) as such an analysis enables the user to find the axes of maximum separation, which in turn facilitates highly accurate identification of unknown analytes.[33] LDA has been used for analysis of a variety of related systems,[34] including colorimetric detection schemes,[35] and is used herein to enable high differentiation between signals that correspond to the different aliphatic alcohol analytes. The input data for LDA was the red, green, and blue (RGB) values of the photographs, which has strong precedence in the colorimetric sensing literature.[36−38] In general, high clustering among points from the same analyte (represented by the same color and shape in Figures 2, 3, 5, and 6) and large amounts of space between the analyte clusters lead to high proportions of total dispersion (values close to 1) and indicates a high-performing system. Less effective clustering within the same group and/or an overlap between the clusters of two different groups leads to lower values for proportion of total dispersion, which in turn leads to a higher ratio of misclassification of unknown analytes.

Optimization of Cyclodextrin. A variety of cyclodextrin hosts was screened with the goal of determining which supramolecular host would provide maximum separation between the analyte-induced color changes, with such separation quantified as the "cumulative proportion of total dispersion." An example of significant dispersion of analyte clusters is shown for 2-HP-*β*-CD (Figure 2C), and a contrasting example with overlapping areas between clusters is shown for Me-*β*-CD (Figure 2B). Using linear discriminant analysis of the RGB data collected from the sample photos, it was determined that the 2-HP-*β*-CD had the highest dispersion using both BODIPY and Rhodamine (dyes **4** and **5**) as color-changing elements with cumulative proportions of total dispersion values of 1.000 and 0.998, respectively (Table 1). Similar trends in the cyclodextrin host were seen with Rhodamine (**5**) (Figure 3) with 2-HP-*β*-CD showing the greatest dispersion (Figure 3C) compared to that of *β*-CD and Me-*β*-CD (Figure 3A,B, respectively).

The higher signal dispersion that was observed when using 2-HP-*β*-CD is likely due to strong binding between the dyes and 2-HP-*β*-CD as well as the high flexibility and water solubility of 2-HP-*β*-CD compared to the other hosts investigated.[39] High binding constants between the alcohol analytes and cyclodextrin hosts increase the strength of interactions between the analyte, host, and dye, resulting in more sensitive analyte-induced signal changes, whereas greater flexibility and water solubility increase the availability of this host to participate in the desired interactions.[40−42] Of note, control experiments conducted in the absence of cyclodextrin resulted in markedly lower dispersion of the signals with significant misclassification of the analytes observed. This was especially true when using Rhodamine as the signal transducing element (75% correct identification of analytes using jackknife classification analysis) but was also decreased using BODIPY (92% correct identification).

Dye Selection. The dyes selected for analysis include highly colored BODIPY (compound **4**) and Rhodamine (compound **5**) analogues. These dyes were selected due to

DOI: 10.1021/acsomega.9b02612
ACS Omega 2019, 4, 18361−18369

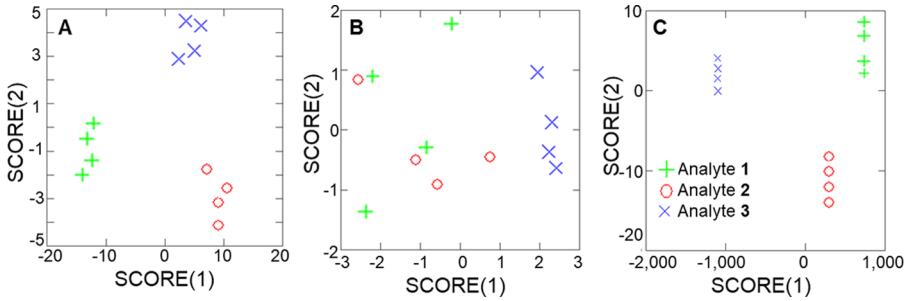

Figure 2. Generated arrays for the detection of ethanol, isopropanol, and methanol with each cyclodextrin supramolecular host using BODIPY (**4**): (A) β-cyclodextrin, (B) methyl-β-cyclodextrin, and (C) 2-hydroxypropyl-β-cyclodextrin.

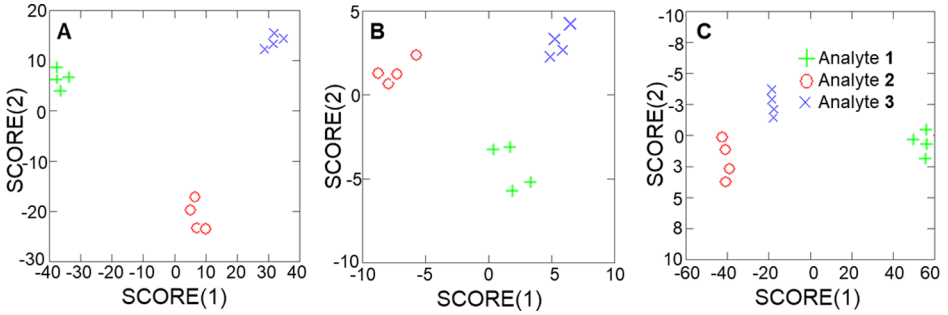

Figure 3. Generated arrays for the detection of ethanol, isopropanol, and methanol with each cyclodextrin supramolecular host using Rhodamine (**5**): (A) β-cyclodextrin, (B) methyl-β-cyclodextrin, and (C) 2-hydroxypropyl-β-cyclodextrin.

Table 1. Cumulative Proportions of Total Dispersion for each Cyclodextrin with Dyes 4 and 5[a]

dye	β-CD	Me-β-CD	2-HP-β-CD
4	0.915	0.986	1.000
5	0.778	0.749	0.998

[a]Values were generated after analysis using SYSTAT 13 LDA software.

their known strong coloration (aligned with their high molar absorptivity coefficients)[43] as well as good aqueous stability[44] and solubility.[45] Moreover, because this system is expected to be used in a wide variety of environments, the toxicity of all components is an important consideration. BODIPY has relatively low toxicity and has been used in a variety of biologically relevant applications;[46,47] while Rhodamine 6G has some toxicity,[48] this toxicity is tunable via judicious choice of counterions,[49] and related dyes have still been used for intracellular applications.[50] As a result, both reported dyes have significant potential in the development of practical detection schemes.

Selection of the Aqueous Environment. All experiments reported herein were conducted in deionized water, although a demonstration of the efficacy of this method in tap water samples would strengthen the applicability of this method. High concentrations of ions in tap water have been reported[51] and include calcium and magnesium ions,[52] which both have been shown to interact with cyclodextrin.[53,54] To measure the general applicability of this method to tap water samples, we conducted experiments using dye **4** in tap water. Results of this experiment indicated somewhat decreased selectivity compared to deionized water, which shows that the tap water components have a deleterious effect on the system performance, although overall 75% correct identification using dye **4** was still observed.

Further insight into the selectivity observed between the alcohol analytes was obtained from computational investigations. Electrostatic potential maps of analytes **1**−**3**, generated using Spartan '18 software, showed significant similarities in the analyte structures with areas of high polarity around the hydroxyl group (Figure 4). Differences between the analytes include noticeable size differences as well as a more

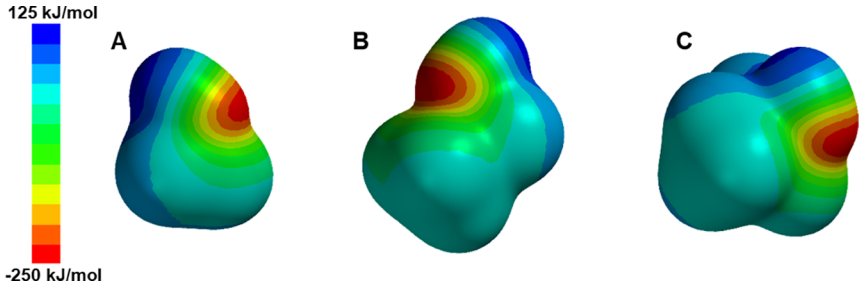

Figure 4. Electrostatic potential maps of (A) methanol, (B) ethanol, and (C) isopropanol. Red areas indicate regions of negative electron density, and blue areas indicate regions of positive electron density. These computations were done using Spartan version 18 computational software.

DOI: 10.1021/acsomega.9b02612
ACS Omega 2019, 4, 18361−18369

concentrated region of positive electron density in methanol compared to the other analytes as shown by the dark blue color. Such differences, combined with steric matching of the analytes with the cyclodextrin cavity and aqueous miscibility of the analytes, contribute to differing binding affinities with the cyclodextrin,[55] resulting in turn in high specificity in the analyte-induced color changes.

Determining the Optimal Concentrations for Testing. In order to determine the optimal analyte concentration to achieve high degrees of analyte-induced separation in the colorimetric responses, the dependence of the LDA plots on analyte concentration was explicitly investigated, and the results are summarized in Table 2. These results indicate that

Table 2. Percent Correct Classification Values Obtained from Jackknife Classification Analysis of the Arrays[a]

dye	0.5 M	1.0 M	2.0 M	3.0 M
4	56	22	67	89
5	67	100	100	78

[a]Values taken after linear discriminant analysis were obtained using SYSTAT version 13 software.

BODIPY was more effective in characterizing data at high analyte concentrations (3.0 M, Figure 5), whereas Rhodamine

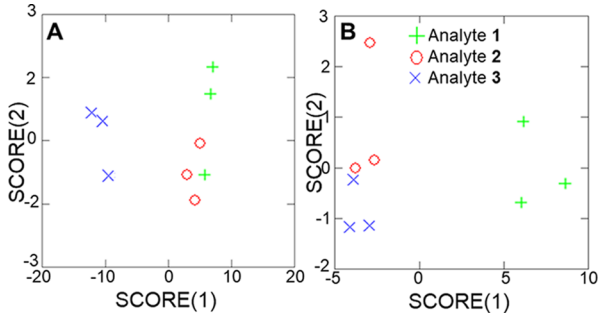

Figure 5. Linear discriminant analysis results obtained at 3.0 M analyte concentration for (A) BODIPY (**4**) and (B) Rhodamine (**5**). All results were obtained using Systat version 13 and following the procedures detailed in the Experimental Section.

provided more dispersed and accurate results between 0.5 M and 2.0 M concentrations (Figure 6). A plausible explanation for these observed results relates to the higher binding constant between BODIPY and 2-HP-β-CD of 3.32×10^5 M^{-1} compared to 1.59×10^5 M^{-1} between Rhodamine and the cyclodextrin. The lower binding constant of Rhodamine allows for better detection at lower alcohol concentrations because the dye is being displaced easier. Because BODIPY binds with a slightly higher binding energy, a higher concentration of alcohol needs to be added to the system in order to displace the dye, causing an overall decrease in system performance. Of note, the fact that the dye is dissolved in isopropanol means that all systems contain a low percentage of this analyte; nonetheless, the markedly higher amounts of analytes added to the solution mean that the isopropanol concentration from the dye solution has a relatively minor effect on the overall signal observed.

Additional computational studies conducted using MOE 2018 software provided important information about the lowest energy docking conformation of each dye with 2-HP-β-CD in a pure water solvent system, and the results are shown

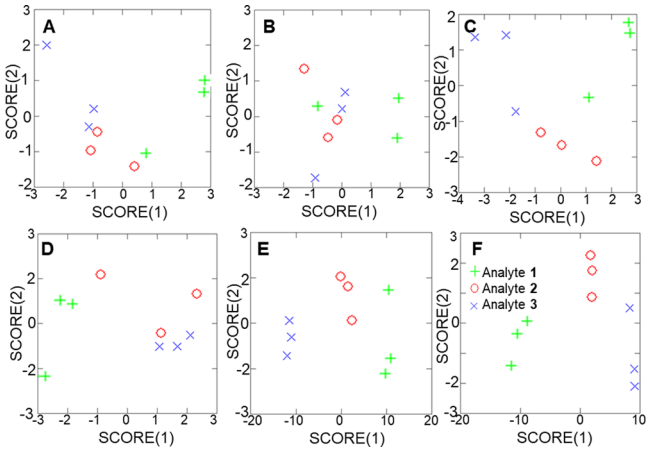

Figure 6. Linear discriminant analysis results generated at lower analyte concentrations. (A) BODIPY (**4**) at 0.5 M concentration of the analyte; (B) BODIPY (**4**) at 1.0 M concentration of the analyte; (C) BODIPY (**4**) at 2.0 M concentration of the analyte; (D) Rhodamine (**5**) at 0.5 M concentration of the analyte; (E) Rhodamine (**5**) at 1.0 M concentration of the analyte; and (F) Rhodamine (**5**) at 2.0 M concentration of the analyte. All results were obtained using Systat version 13 and following the procedures detailed in the Experimental Section.

in Figure 7. Of note, BODIPY (**4**) exhibited markedly more inclusion in the cyclodextrin host compared to Rhodamine (**5**) with a substantial portion of the Rhodamine remaining exposed to the solvent. This solvent-exposed area of Rhodamine has a greater ability to interact with the analyte in solution. This result implies that dye displacement by the alcohol may not be necessary to effect a color change if the alcohol and dye interact via the solvent-accessible portion. Such interactions are not dependent on the binding constant of the dyes in cyclodextrin and provide an additional mechanism by which the system can lead to analyte-specific color changes. Efforts to investigate the extent to which either or both mechanisms (i.e., dye displacement from the cavity and/or interactions between the dye and analyte through solvent-exposed areas) are operative in this system are currently underway in our laboratory.

Moreover, the addition of the alcohol analyte to the solution of dye in cyclodextrin had measurable changes on the supramolecular complex. In particular, computational results indicated that adding methanol to a solution of BODIPY in 2-HPCD resulted in the weakening of the association between BODIPY and 2-HPCD and strengthening of the affinity of the BODIPY for the solvent (Figure 8). This result supports that colorimetric changes induced by the addition of the alcohol analyte are a result of decreased affinity of the dye for the hydrophobic cyclodextrin cavity.

Determining the LOD and LOQ for the Analytes with Dyes 4 and 5. In addition to measuring the ability of the system to differentiate between structurally similar analytes, the sensitivity of the system to low analyte concentrations was also investigated. For these experiments, the green value of the photographs was taken to represent the signal output as our results indicate that this is the signal that changes most significantly in response to the changing concentration of the analyte. These results are summarized in Tables 3 (for 0.127 mM BODIPY and 0.093 mM Rhodamine) and 4 (for 0.382 mM BODIPY and 0.280 mM Rhodamine) and indicate that analyte concentrations as low as 0.2 mM were detectable via

DOI: 10.1021/acsomega.9b02612
ACS Omega 2019, 4, 18361−18369

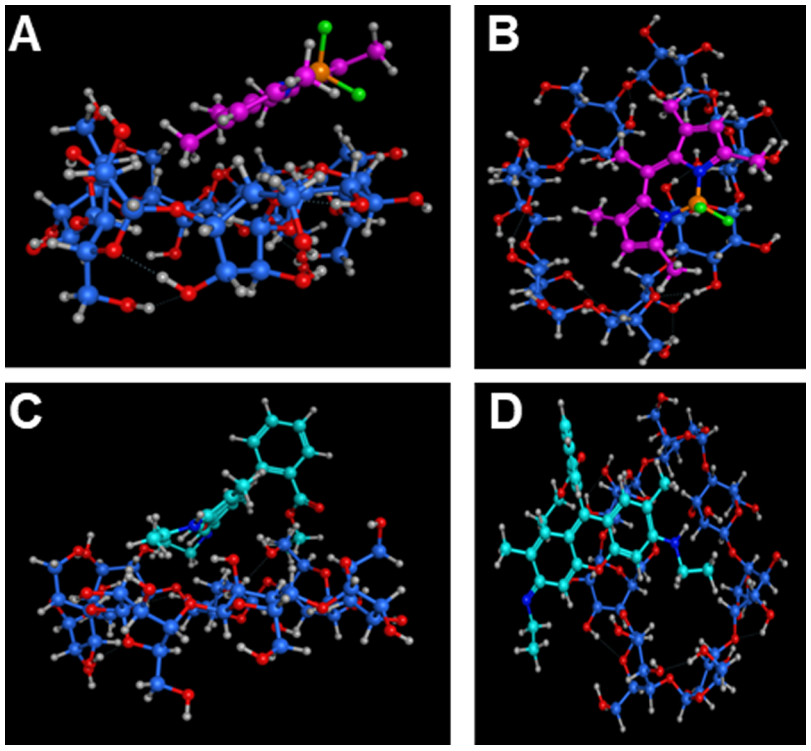

Figure 7. Lowest energy conformations of BODIPY (**4**) and Rhodamine (**5**) in 2-HP-β-CD. (A) Side view of the complex with BODIPY (**4**). (B) Aerial view of the complex with BODIPY (**4**). (C) Side view of the complex with Rhodamine (**5**). (D) Aerial view of the complex with Rhodamine (**5**). Color coding: for the cyclodextrin host, the dark blue color represents the carbon atoms, the red color represents the oxygen atoms, and the gray color represents hydrogen atoms. For BODIPY, the purple color represents carbon atoms, gray represents hydrogen, blue represents nitrogen, orange represents boron, and green represents fluorine. For Rhodamine, the teal color represents carbon, gray represents hydrogen, red represents oxygen, and dark blue represents nitrogen.

this method (for isopropanol, using relatively high concentrations of Rhodamine). Compared to the LODs reported in Table 3, there was no significant decrease in the LODs observed with BODIPY at higher concentrations. In contrast, the Rhodamine trial showed much better improvement at higher dye concentrations with a 48% decrease in the LOD and a decrease of 68% in the LOQ value. These marked changes are in line with the higher solvent and analyte accessibility displayed by Rhodamine (vide supra) and indicate substantial promise in the further optimization of sensitive alcohol sensors. An example of a color array that illustrates the visible color change of BODIPY in the presence of isopropanol is shown in Figure 9.

Of note, visible color changes were present in both dye **4** and dye **5** trials. When using dye **4**, the visible color change is seen going from a dull orange when no alcohol is present to a bright yellow after all additions, as can be seen in Figure 9. The stock solution of this dye, prepared in isopropanol, is bright fluorescent green. In the dye **5** trials, the initial color is a bright orange that also becomes a bright yellow after the analyte is added.

CONCLUSIONS

Harnessing the highly specific complexation of small-molecule guests inside supramolecular cyclodextrin hosts provides a fundamentally unique system for the detection of those guests. Reported herein is the application of such host–guest complexes for the colorimetric detection of alcohols using highly practical, easily available materials to achieve excellent selectivity (100% differentiation) and moderate sensitivity (as low as 0.2 M). Computational experiments involving the cyclodextrin, analytes, and highly colored dyes are invoked to explain the underlying basis of this strong analyte specificity as remarkably structurally similar analytes leading to noticeably different colorimetric read-out signals. Efforts to improve the sensitivity, broaden the scope of such detection, and develop sensors for mixtures of alcohols without requiring additional separation procedures (in accordance with literature reports of analogous systems)[56] are currently underway in our laboratory, and results of these and other investigations will be reported in due course.

EXPERIMENTAL SECTION

Materials and Methods. The alcohol analytes **1**–**3** and dyes **4** and **5** shown in Figure 1 were obtained from the Millipore-Sigma chemical company, and the cyclodextrins were obtained from the Tokyo Chemical Industry (TCI) chemical company. All chemicals were used as received. All aqueous solutions were made in glass jars and transferred to 50 mL white, polypropylene cups that had previously been used in a Keurig machine and were washed thoroughly prior to usage. A plastic container (with dimensions 21 cm × 15 cm × 7 cm) was spray-painted using Krylon Fusion Satin Black spray paint to limit ambient light, and a 1.5 cm × 1.5 cm hole was cut in the center of the lid to enable photography of the solution. An additional polypropylene cup previously used for a Keurig machine was positioned under the opening and secured to the bottom of the container with electrical tape. Two strips of LED white light tape (purchased from The Home Depot, with a voltage of 12, a watt equivalence of 8.5, and an actual color

DOI: 10.1021/acsomega.9b02612
ACS Omega 2019, 4, 18361−18369

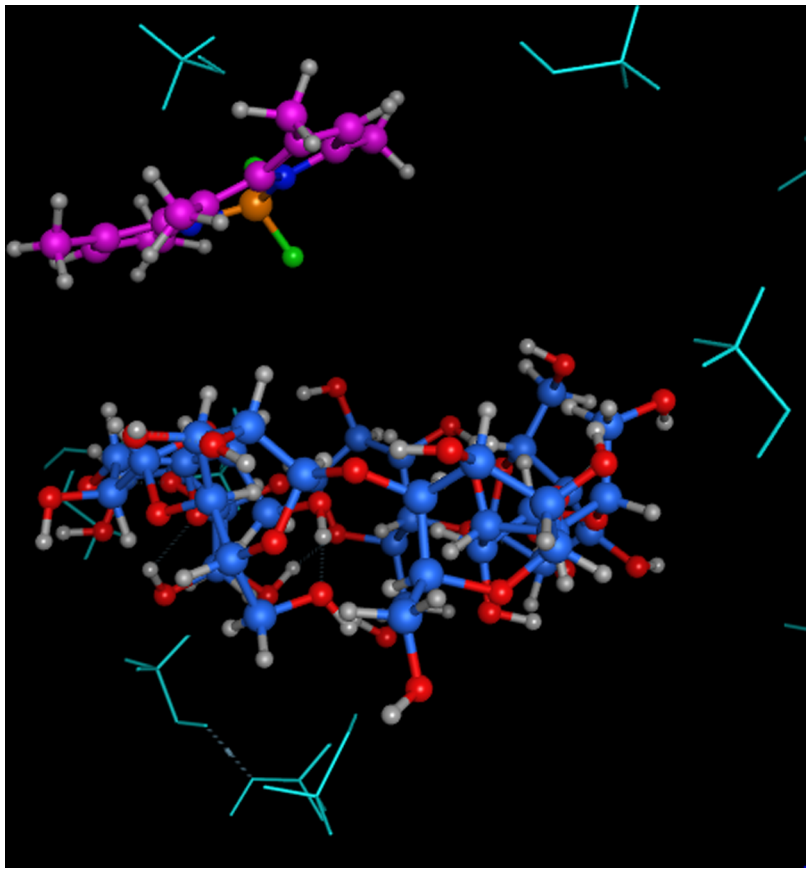

Figure 8. Lowest energy conformations of BODIPY (**4**) in 2-HP-*β*-CD following the introduction of methanol. The methanol is modeled as teal stick figures, and the colors of the BODIPY and cyclodextrin are identical to the colors used in Figure 7.

Table 3. LODs and LOQs of Each Alcohol with Dyes 4 and 5 in the Presence of 2-HP-*β*-CD

dye	alcohol	LOD (M)[a]	LOQ (M)[b]
4	isopropanol	0.319	0.805
	ethanol	0.491	1.74
	methanol	0.249	0.823
5	isopropanol	0.386	1.05
	ethanol	0.216	0.442
	methanol	0.331	0.730

[a]Values calculated according to eq 1 and the equation of the line of best fit for each dye−alcohol complex. [b]Values calculated according to eq 2 and the equation of the line of best fit for each dye−alcohol complex.

Table 4. LODs and LOQs of Isopropanol with Increased Concentrations of Dyes 4 and 5 and 2-HP-*β*-CD

dye	LOD (M)	LOQ (M)
4	0.3170 (0.50%)[a]	0.7812 (3.0%)
5	0.2004 (48%)	0.3341(68%)

[a]Number in parentheses represents the percent change, which is, in all cases, a decrease from the LOD values obtained in Table 3 to the ones calculated using a higher concentration of the dye in solution.

temperature of 4000 K) were placed on the interior of the container, on all sides of the container, to provide uniform sample illumination. An annotated figure of the lightbox can be found in the Supporting Information. The cup that contained the sample was placed into the secured cup prior to imaging.

Figure 9. Colorimetric array of the 60 samples from the trial using dye **4** and analyte **3**. The concentration of the analyte increases from left to right.

Photographs of the solutions were taken from 2.0 cm above the top of the sample cup with a Samsung Galaxy S8+ (model number: G950U) in the manual mode with the following settings: ISO set to 100, aperture set to 1/350, macro-focused (close-up focus), and the white balance set at 5500 K. These settings were kept constant for all trials to avoid variation in color capture. Preliminary work that varied the smartphone camera settings led to changes in the RGB values obtained with automatic settings, leading to reduced consistency between trials and even within the same trial. Similar challenges in consistency were observed without using LED lights for consistent sample illumination. Using the manual mode in both the smartphone and LED lights around the sample solved the consistency challenges and enabled accurate and reproducible results to be obtained. Images were processed with ImageJ software to measure the red, green, and blue values (RGB) of the solutions following the procedures detailed below.

General Procedure for Making Stock Solutions. Three 250 mL solutions of *β*-cyclodextrin (*β*-CD), methyl-*β*-

DOI: 10.1021/acsomega.9b02612
ACS Omega 2019, 4, 18361−18369

cyclodextrin (Me-β-CD), and 2-hydroxypropyl-β-cyclodextrin (2-HP-β-CD) cyclodextrin were made at relatively high concentrations (Table 5). The stock solutions for BODIPY and Rhodamine dyes were made in isopropanol at concentrations of 3.80 mM and 2.08 mM, respectively (1 mg/mL for each dye). Diluted dye solutions were prepared by adding 5.0 mL of the concentrated stock solutions to a 150 mL volumetric flask and diluting to the mark with water.

Table 5. Concentration of Cyclodextrins and Dyes in Solution[a]

solute	solvent	concentration (mM)
β-CD	DI H_2O	16.5
Me-β-CD	DI H_2O	9.69
2-HP-β-CD	DI H_2O	2.39
BODIPY (**4**)	isopropanol	3.82
Rhodamine (**5**)	isopropanol	2.08

[a]The final solution concentrations were calculated based on the amounts of solute and solvent added. See text for more information.

General Procedure for the Optimization of the Supramolecular Cyclodextrin Host. In a glass sample jar, 10.00 mL of a β-CD stock solution was combined with 10.00 mL of one of the diluted dye solutions. This mixture was manually shaken for 1 min to ensure thorough mixing. After mixing, 5.00 mL of the alcohol was added. This mixture was transferred to the sample cup and placed in the lightbox. The cover was placed on, and a photo was taken using the smartphone with the settings listed above. This procedure was repeated for Me-β-CD and 2-HP-β-CD with both dyes and each of the three alcohols (18 total samples). Four trials of each sample were completed with a calculated average standard deviation in red, green, and blue values of 0.08, 0.14, and 1.99%, respectively.

General Procedure for the Optimization of Analyte Concentration. Preparation of the cyclodextrin−dye solution was performed following the procedures detailed above with 2-HP-β-CD used as the host. A 0.5 M solution of the alcohol was made by adding alcohol to the cyclodextrin−dye solution in the glass jar with additional samples tested for each alcohol at a variety of concentrations (0.5, 1.0, 2.0, and 3.0 M) using the BODIPY and Rhodamine dyes (8 samples, 3 trials each). These solutions were transferred to a sample cup and placed in the lightbox, and a photo was taken of every sample.

General Procedure for Calculating the Limits of Detection (LOD) and Limits of Quantification (LOQ). The limit of detection (LOD), defined as the lowest concentration of the analyte that can be detected, was obtained using the calibration curve method, following procedures reported by Loock and co-workers.[57] The limit of detection of the blank (LOD_{blank}) is defined according to eq 1 below

$$LOD_{blank} = m_{blank} + 3(SD_{blank}) \quad (1)$$

where m is the average of the values obtained from the blank sample and SD is the standard deviation of those measurements. The limit of quantification (LOQ) is the lowest concentration of the analyte that can be quantified.[58] The limit of quantification of the blank is defined according to eq 2 below

$$LOQ_{blank} = m_{blank} + 10(SD_{blank}) \quad (2)$$

where m is the average of the values obtained from the blank sample and SD is the standard deviation of those measurements.

Preparation of the cyclodextrin−dye solution was performed as mentioned above using 2-HP-β-CD as the optimized supramolecular host. This solution was transferred to the sample cup and placed in the spray-painted box. A photograph was taken in order to obtain the blank measurement of the solution in the absence of any alcohol. Using a 20−200 μL Fisherbrand Elite micropipette, 100 μL of the alcohol was added, and a picture was taken. These 100 μL additions continued until 6.0 mL of the alcohol had been added to the solution. This process was repeated three times for each alcohol and in the presence of each dye. The RGB values of the solution were used to determine the level of detection of each alcohol in both dyes.

General Procedure for Obtaining RGB Values. Photos were cropped to be the same 500 × 500 pixel ratio focused on the center of the sample (using https://www.birme.net) to ensure that the area of the picture that was being measured was consistent across all samples. These images were processed using the RGB measurement tool plug-in that is available for ImageJ software. More details of these procedures can be found in the Supporting Information of this manuscript.

General Procedure for Conducting Linear Discriminant Analyses. SYSTAT 13 statistical computing software was used to quantify the degree of separation of color change in the solutions using the following settings for linear discriminant analysis (LDA): (a) Classical Discriminant Analysis; (b) Grouping Variable: Analytes (alcohols); (c) Predictors: Red, Green, and Blue; and (d) Long-Range Statistics: Mahal.

General Procedure for Computational Modeling. Spartan version '18 was used to calculate the equilibrium values for the analytes in their ground-state electric potential surfaces using a semi-empirical PM3 model for each analyte. Molecular Operating Environment 2018 (MOE) was used to do the docking studies for each dye, alcohol analyte, and 2-HP-β-CD host. A general energy minimization was performed using the "quick prep" function on the software. For the docking studies, the set of atoms defined as the receptor was both 2-HP-β-CD and the solvent so that the dye could move freely in the system. Placement was done using the Triangle Matches method with the London Dispersion dG score in 30 poses. Refinement was done using the Rigid Receptor method with the GBVI/WSA dG score in 5 poses. This generated the docking of the dye−cyclodextrin complex with the lowest energy conformation. Summary figures generated from these procedures can be found in the Supporting Information of this manuscript.

■ ASSOCIATED CONTENT

Supporting Information

The Supporting Information is available free of charge on the ACS Publications website at DOI: 10.1021/acsomega.9b02612.

Experimental details of all analytes, dyes, and hosts; details of lightbox construction; optimization of analyte concentrations and supramolecular host; determination of array-based selectivity, computational modeling, and limits of detection and quantification; and all summary tables and figures (PDF)

DOI: 10.1021/acsomega.9b02612
ACS Omega 2019, 4, 18361−18369

AUTHOR INFORMATION

Corresponding Author

*E-mail: mindy.levine@gmail.com; m_levine@uri.edu. Phone: 401-874-4243. Fax: 401-874-5072.

ORCID

Mindy Levine: 0000-0003-4847-7791

Present Address

§Present address: Ari'el University, 65 Ramat HaGolan Street, Ari'el, Israel.

Author Contributions

The manuscript was written through contributions of all authors. All authors have given approval to the final version of the manuscript.

Notes

The authors declare no competing financial interest.

ACKNOWLEDGMENTS

The authors wish to thank Mr. Benjamin Cromwell for his support in setting up and analyzing the computational components and the MAGIC (More Active Girls in Computing) mentoring program for connecting P.H. with Levine and co-workers and the associated research.

REFERENCES

(1) Verma, A.; Ambatipudi, K. Challenges and Opportunities of Bovine Milk Analysis by Mass Spectrometry. *Clin. Proteomics* **2016**, *13*, 8−13.

(2) Háda, V.; Bagdi, A.; Bihari, Z.; Timári, S. B.; Fizil, Á.; Szántay, C., Jr. Recent Advancements, Challenges, and Practical Considerations in the Mass Spectrometry-Based Analytics of Protein Biotherapeutics: A Viewpoint from the Biosimilar Industry. *J. Pharm. Biomed. Anal.* **2018**, *161*, 214−238.

(3) Huang, X.; Xu, D.; Chen, J.; Liu, J.; Li, Y.; Song, J.; Ma, X.; Guo, J. Smartphone-Based Analytical Biosensors. *Analyst* **2018**, *143*, 5339−5351.

(4) DiScenza, D. J.; Culton, E.; Verderame, M.; Lynch, J.; Serio, N.; Levine, M. Towards Rational Chemosensor Design through Improved Understanding of Experimental Parameter Variation and Tolerance in Cyclodextrin-Promoted Fluorescence Detection. *Chemosensors* **2017**, *5*, 34−34/15.

(5) Serio, N.; Miller, K.; Levine, M. Efficient Detection of Polycyclic Aromatic Hydrocarbons and Polychlorinated Biphenyls via Three-Component Energy Transfer. *Chem. Commun.* **2013**, *49*, 4821−4823.

(6) Serio, N.; Moyano, D. F.; Rotello, V. M.; Levine, M. Array-Based Detection of Persistent Organic Pollutants via Cyclodextrin Promoted Energy Transfer. *Chem. Commun.* **2015**, *51*, 11615−11618.

(7) DiScenza, D. J.; Levine, M. Sensitive and Selective Detection of Alcohols via Fluorescence Modulation. *Supramol. Chem.* **2016**, *28*, 881−891.

(8) Chaudhuri, S.; DiScenza, D. J.; Verderame, M.; Cromwell, B.; Levine, M. Colorimetric Detection of Polycyclic Aromatic Hydrocarbons using Supramolecular Cyclodextrin Dimer-Squaraine Constructs. *Supramol. Chem.* **2019**, *31*, 211−219.

(9) Ma, X.; He, S.; Qiu, B.; Luo, F.; Guo, L.; Lin, Z. Noble Metal Nanoparticle-Based Multicolor Immunoassays: An Approach toward Visual Quantification of the Analytes with the Naked Eye. *ACS Sens.* **2019**, *4*, 782−791.

(10) Kangas, M. J.; Burks, R. M.; Atwater, J.; Lukowicz, R. M.; Williams, P.; Holmes, A. E. Colorimetric Sensor Arrays for the Detection and Identification of Chemical Weapons and Explosives. *Crit. Rev. Anal. Chem.* **2017**, *47*, 138−153.

(11) Li, Z.; Zhang, S.; Yu, T.; Dai, Z.; Wei, Q. Aptamer-Based Fluorescent Sensor Array for Multiplexed Detection of Cyanotoxins on a Smartphone. *Anal. Chem.* **2019**, *91*, 10448−10457.

(12) Li, Y.; Wang, Z.; Sun, L.; Liu, L.; Xu, C.; Kuang, H. Nanoparticle-Based Sensors for Food Contaminants. *TrAC, Trends Anal. Chem.* **2019**, *113*, 74−83.

(13) Zhou, Y.; Ding, L.; Wu, Y.; Huang, X.; Lai, W.; Xiong, Y. Emerging Strategies to Develop Sensitive AuNP-Based ICTS Nanosensors. *TrAC, Trends Anal. Chem.* **2019**, *112*, 147−160.

(14) Woźniak, M. K.; Wiergowski, M.; Namieśnik, J.; Biziuk, M. Biomarkers of Alcohol Consumption in Body Fluids - Possibilities and Limitations of Application in Toxicological Analysis. *Curr. Med. Chem.* **2019**, *26*, 177−196.

(15) Casini, B.; Righi, A.; De Feo, N.; Totaro, M.; Giorgi, S.; Zezza, L.; Valentini, P.; Tagliaferri, E.; Costa, A. L.; Barnini, S.; Baggiani, A.; Lopalco, P. L.; Malacarne, P.; Privitera, G. P. Improving Cleaning and Disinfection of High-Touch Surfaces in Intensive Care During Carbapenem-Resistant Acinetobacter baumannii Endemo-Epidemic Situations. *Int. J. Environ. Res. Public Health* **2018**, *15*, 2305.

(16) Cheng, W.-H.; Huang, H.-L.; Chen, K.-S.; Chang, Y.-J. Quantification of VOC Emissions from Paint Spraying on a Construction Site Using Solid Phase Microextraction Devices. *J. Environ. Sci. Health A* **2017**, *52*, 1158−1163.

(17) Rogula-Kopiec, P.; Rogula-Kozłowska, W.; Pastuszka, J. S.; Mathews, B. Air Pollution of Beauty Salons by Cosmetics from the Analysis of Suspensed Particulate Matter. *Environ. Chem. Lett.* **2019**, *17*, 551−558.

(18) Gorinstein, S.; Trakhtenberg, S. Alcohol Beverages and Biochemical Changes in Blood. *Addict. Biol.* **2003**, *8*, 445−454.

(19) Pradhan, B.; Hadengue, A.; Chappuis, F.; Chaudhary, S.; Baral, D.; Gache, P.; Karki, P.; Rijal, S. Alcoholic Liver Disease in Nepal: Identifying Homemade Alcohol as a Culprit. *Clin. Exp. Gastroenterol.* **2015**, *8*, 183−189.

(20) Janagama, H. K.; Mai, T.; Han, S.; Nadala, L.; Nadala, C.; Samadpour, M. Dipstick Assay for Rapid Detection of Beer Spoilage Organisms. *J. AOAC Int.* **2018**, *101*, 1913−1919.

(21) Teshome, D. A.; Rainer, M.; Noel, J.-C.; Schüßler, G.; Fuchs, D.; Bliem, H. R.; Günther, B. K. Chemical Compositions of Traditional Alcoholic Beverages and Consumers' Characteristics, Ethiopia. *African J. Food Sci.* **2017**, *11*, 234−245.

(22) Barreto, S. G.; Saccone, G. T. P. Alcohol-Induced Acute Pancreatitis: The Critical Mass' Concept. *Med. Hypotheses* **2010**, *75*, 73−76.

(23) Renger, R. S.; Van Hateren, S. H.; Luyben, K. C. A. M. The Formation of Esters and Higher Alcohols During Brewery Fermentation; The Effect of Carbon Dioxide Pressure. *J. Inst. Brew.* **1992**, *98*, 509−13.

(24) Liu, L.; Chen, M.; Zhao, L.; Zhao, Q.; Hu, R.; Zhu, J.; Yan, R.; Dai, K. Ethanol Induces Platelet Apoptosis. *Alcohol.: Clin. Exp. Res.* **2017**, *41*, 291−298.

(25) Lindberg, L.; Grubb, D.; Dencker, D.; Finnhult, M.; Olsson, S.-G. Detection of Mouth Alcohol During Breath Alcohol Analysis. *Forensic Sci. Int.* **2015**, *249*, 66−72.

(26) Boumba, V. A.; Kourkoumelis, N.; Gousia, P.; Economou, V.; Papadopoulou, C.; Vougiouklakis, T. Modeling Microbial Ethanol Production by E. Coli under Aerobic/Anaerobic Conditions: Applicability to Real Postmortem Cases and to Postmortem Blood Derived Microbial Cultures. *Forensic Sci. Int.* **2013**, *232*, 191−198.

(27) Galpothdeniya, W. I. S.; Regmi, B. P.; McCarter, K. S.; de Rooy, S. L.; Siraj, N.; Warner, I. M. Virtual Colorimetric Sensor Array: Single Ionic Liquid for Solvent Discrimination. *Anal. Chem.* **2015**, *87*, 4464−4471.

(28) Yu, Y.; Ma, J.-P.; Zhao, C.-W.; Yang, J.; Zhang, X.-M.; Liu, Q.-K.; Dong, Y.-B. Copper(I) Metal-Organic Framework: Visual Sensor for Detecting Small Polar Aliphatic Volatile Organic Compounds. *Inorg. Chem.* **2015**, *54*, 11590−11592.

(29) Guo, Y.; Xue, S.; Dìrtu, M. M.; Garcia, Y. A Versatile Iron(II)-Based Colorimetric Sensor for the Vapor-Phase Detection of Alcohols and Toxic Gases. *J. Mater. Chem. C* **2018**, *6*, 3895−3900.

(30) Munaf, E.; Zein, R.; Jin, J.-Y.; Takeuchi, T. Liquid Chromatographic Determination of Alcohols in Food and Beverages

DOI: 10.1021/acsomega.9b02612
ACS Omega 2019, 4, 18361−18369

with Indirect Polarimetric Detection Using a β-Cyclodextrin Mobile Phase. *Anal. Sci.* **2002**, *18*, 903−906.
(31) Wang, C.; Chen, F.; He, X.-w.; Kang, S.-z.; You, C.-c.; Liu, Y. Cyclodextrin Derivative-Coated Quartz Crystal Microbalances for Alcohol Sensing and Application as Methanol Sensors. *Analyst* **2001**, *126*, 1716−1720.
(32) Wang, H.; Yang, L.; Chu, S.; Liu, B.; Zhang, Q.; Zou, L.; Yu, S.; Jiang, C. Semiquantitative Visual Detection of Lead Ions with a Smartphone via a Colorimetric Paper-Based Analytical Device. *Anal. Chem.* **2019**, *91*, 9292−9299.
(33) Esteki, M.; Shahsavari, Z.; Simal-Gandara, J. Use of Spectroscopic Methods in Combination with Linear Discriminant Analysis for Authentication of Food Products. *Food Control* **2018**, *91*, 100−112.
(34) Gade, A. M.; Meadows, M. K.; Ellington, A. D.; Anslyn, E. V. Differential Array Sensing for Cancer Cell Classification and Novelty Detection. *Org. Biomol. Chem.* **2017**, *15*, 9866−9874.
(35) Fahimi-Kashani, N.; Hormozi-Nezhad, M. R. Gold-Nanoparticle-Based Colorimetric Sensor Array for Discrimination of Organophosphate Pesticides. *Anal. Chem.* **2016**, *88*, 8099−8106.
(36) Wang, T.-T.; Lio, C. K.; Huang, H.; Wang, R.-Y.; Zhou, H.; Luo, P.; Qing, L.-S. A Feasible Image-Based Colorimetric Assay Using a Smartphone RGB Camera for Point-of-Care Monitoring of Diabetes. *Talanta* **2020**, *206*, 120211.
(37) Huang, Y.; Cheng, P.; Tan, C. Visual Artificial Tongue for Identification of Various Metal Ions in Mixtures and Real Water Samples: A Colorimetric Sensor Array Using Off-the-Shelf Dyes. *RSC Adv.* **2019**, *9*, 27583−27587.
(38) Sajed, S.; Arefi, F.; Kolahdouz, M.; Sadeghi, M. A. Improving Sensitivity of Mercury Detection Using Learning Based Smartphone Colorimetry. *Sens. Actuators, B: Chem.* **2019**, *298*, 126942.
(39) Liu, J.; Liu, G.; Liu, W.; Wang, Y.; Xu, M.; Wang, B. Turn-On Fluorometric β-Carotene Assay Based on Competitive Host-Guest Interaction between Rhodamine 6G and β-Carotene with a Graphene Oxide Functionalized with a β-Cyclodextrin-Modified Polyethyleneimine. *Microchim. Acta* **2016**, *183*, 1161−1168.
(40) Maitre, M. M.; Longhi, M. R.; Granero, G. G. Ternary Complexes of Flurbiprofen with HP-β-CD and Ethanolamines Characterization and Transdermal Delivery. *Drug Dev. Ind. Pharm.* **2007**, *33*, 311−326.
(41) Zhang, H.; Ge, C.; van der Spoel, D.; Feng, W.; Tan, T. Insight into the Structural Deformations of β-Cyclodextrin Caused by Alcohol Cosolvents and Guest Molecules. *J. Phys. Chem. B* **2012**, *116*, 3880−3889.
(42) Boonyarattanakalin, K.; Viernstein, H.; Wolschann, P.; Lawtrakul, L. Influence of Ethanol as a Co-Solvent in Cyclodextrin Inclusion Complexation: A Molecular Dynamics Study. *Sci. Pharm.* **2015**, *83*, 387−399.
(43) Hatamimoslehabadi, M.; Bellinger, S.; La, J.; Ahmad, E.; Frenette, M.; Yelleswarapu, C.; Rochford, J. Correlation of Photophysical Properties with the Photoacoustic Emission for a Selection of Established Chromophores. *J. Phys. Chem. C* **2017**, *121*, 24168−24178.
(44) Rumyantsev, E. V.; Alyoshin, S. N.; Marfin, Y. S. Kinetic Study of Bodipy Resistance to Acids and Alkalis: Stability Ranges in Aqueous and Non-Aqueous Solutions. *Inorg. Chim. Acta* **2013**, *408*, 181−185.
(45) Cheng, C.-C.; Chiu, T.-W.; Yang, X.-J.; Huang, S.-Y.; Fan, W.-L.; Lai, J.-Y.; Lee, D.-J. Self-Assembling Supramolecular Polymer Membranes for Highly Effective Filtration of Water-Soluble Fluorescent Dyes. *Polym. Chem.* **2019**, *10*, 827−834.
(46) Gao, Y.; Pan, Y.; Chi, Y.; He, Y.; Chen, H.; Nemykin, V. N. A ″Reactive″ Turn-on Fluorescence Probe for Hypochlorous Acid and its Bioimaging Application. *Spectrochim. Acta, Part A: Molec. Biomolec. Spectroscopy* **2019**, *206*, 190−196.
(47) Ogle, M. M.; Smith McWilliams, A. D.; Ware, M. J.; Curley, S. A.; Corr, S. J.; Martí, A. A. Sensing Temperature in Vitro and in Cells Using a BODIPY Molecular Probe. *J. Phys. Chem. B* **2019**, *123*, 7282−7289.
(48) Chaudhary, S.; Kaur, Y.; Umar, A.; Chaudhary, G. R. 1-Butyl-3-methylimidazolium Tetrafluoroborate Functionalized ZnO Nanoparticles for Removal of Toxic Organic Dyes. *J. Mol. Liq.* **2016**, *220*, 1013−1021.
(49) Magut, P. K. S.; Das, S.; Fernand, V. E.; Losso, J.; McDonough, K.; Naylor, B. M.; Aggarwal, S.; Warner, I. M. Tunable Cytotoxicity of Rhodamine 6G via Anion Variations. *J. Am. Chem. Soc.* **2013**, *135*, 15873−15879.
(50) Bhowmick, R.; Alam, R.; Mistri, T.; Bhattacharya, D.; Karmakar, P.; Ali, M. Morphology-Directing Synthesis of Rhodamine-Based Fluorophore Microstructures and Application toward Extra- and Intracellular Detection of Hg^{2+}. *ACS Appl. Mater. Interfaces* **2015**, *7*, 7476−7485.
(51) Velizarov, S.; Crespo, J. G.; Reis, M. A. Removal of Inorganic Anions from Drinking Water Supplies by Membrane Bio/Processes. *Rev. Environ. Sci. Bio/Technol.* **2004**, *3*, 361−380.
(52) Jain, C. K.; Vaid, U. Assessment of Groundwater Quality for Drinking and Irrigation Purposes Using Hydrochemical Studies in Nalbari District of Assam, India. *Environ. Earth Sci.* **2018**, *77*, 254.
(53) Angelova, S.; Nikolova, V.; Molla, N.; Dudev, T. Factors Governing the Host-Guest Interactions between IIA/IIB Group Metal Cations and α-Cyclodextrin: A DFT/CDM Study. *Inorg. Chem.* **2017**, *56*, 1981−1987.
(54) Sumithra, M.; Sivaraj, R.; Selvan, G. T.; Selvakumar, P. M.; Enoch, I. V. M. V. Ca^{2+} Ion Sensing by a Piperidin-4-one Derivative and the Effect of β-Cyclodextrin Complexation on the Sensing. *J. Luminescence* **2017**, *185*, 205−211.
(55) Yoshikiyo, K.; Matsui, Y.; Yamamoto, T. Determination of Binding Constants for Inclusion Complexes of Cyclodextrins with Organic Solvents, Ethylene Glycol, and its Related Compounds by Means of ^{1}H NMR Spectroscopy. *Bull. Chem. Soc. Jpn* **2012**, *85*, 1206−1209.
(56) Li, Z.; Askim, J. R.; Suslick, K. S. The Optoelectronic Nose: Colorimetric and Fluorometric Sensor Arrays. *Chem. Rev.* **2019**, *119*, 231−292.
(57) Loock, H.-P.; Wentzell, P. D. Detection Limits of Chemical Sensors: Applications and Misapplications. *Sens. Actuators B: Chem.* **2012**, *173*, 157−163.
(58) Belter, M.; Sajnóg, A.; Barałkiewicz, D. Over a Century of Detection and Quantification Capabilities in Analytical Chemistry - Historical Overview and Trends. *Talanta* **2014**, *129*, 606−616.

DOI: 10.1021/acsomega.9b02612
ACS Omega 2019, 4, 18361−18369